Synthesis, Physicochemical Properties, and Evaluation of N-Substituted-2-alkyl-3-hydroxy-4(1H)-pyridinones[†]

Bijaya L. Rai, Lotfollah S. Dekhordi, Hicham Khodr, Yi Jin, Zudong Liu, and Robert C. Hider*

Department of Pharmacy, King's College London, Manresa Road, London SW3 6LX, U.K., and Novartis, Pharmaceuticals Research, CH-4002 Basel, Switzerland

Received November 14, 1997

The synthesis of a range of 3-hydroxy-4(1H)-pyridinones with potential for the chelation of iron(III) is described. The pK_a values of respective ligands and the stability constants of their iron(III) complexes are presented. The distribution coefficient values of a range of 48 hydroxypyridinones and their corresponding iron(III) complexes between 1-octanol and MOPS buffer (pH 7.4) are reported. The range of log $D_{complex}$ values covers 7 orders of magnitude. The results suggest the existence of a biphasic relationship between the distribution coefficient values of the chelator and the corresponding iron(III) complexes. For ligands with a log D_{ligand} = −1, a linear relationship exists with a value of the slope 2.53, whereas with ligands with a log D_{ligand} < −1, a linear relationship exists with a slope of 0.49. The reduced slope for the more hydrophilic molecules of the series offers some advantage for this type of hydroxypyridinone as the distribution coefficients for such complexes do not change so rapidly with increasing ligand hydrophilicity. The ability of selected 3-hydroxypyridinones to facilitate the excretion of iron in bile was investigated in non-iron-overloaded, bile duct-cannulated rats and in a [^{59}Fe]ferritin-loaded rat model. Both systems compare the ability of chelators to remove iron from the liver, the prime target organ in thalassemia. The N-(hydroxyalkyl)-3-hydroxy-pyridin-4-ones are demonstrated to be orally active under the in vivo conditions adopted. Thus both 1-(hydroxyalkyl)- and 1-(carboxyalkyl)pyridinones are able to remove iron from the liver. Although 1-(carboxyalkyl)hydroxypyridinones are active, they do not demonstrate any clear advantage over Deferiprone (1,2-dimethyl-3-hydroxypyridin-4-one). Indeed 1-(hydroxyalkyl)-hydroxypyridinones which are known to be rapidly converted to 1-(carboxyalkyl)hydroxypyridinones are also marginally superior to Deferiprone. In contrast, 2-ethyl-1-(2′-hydroxyethyl)-3-hydroxypyridin-4-one, which is not metabolized to the corresponding (carboxyalkyl)-hydroxypyridinone, was found to be superior to Deferiprone and therefore deserves further consideration as an orally active iron chelator with potential for the treatment of iron overload associated with transfusion-dependent thalassemia.

Iron possesses two oxidation states, iron(II) and iron(III), which are relatively stable under most biological conditions. The redox potential between these two states can be adjusted such that oxidation processes centered on iron can be readily coupled to metabolic reactions. Furthermore, iron has a high affinity for oxygen atoms. These two properties are widely utilized by iron-containing proteins. However, these same two properties render iron potentially toxic, particularly when the metal is nonspecifically bound to proteins and membranes. Under aerobic conditions, such iron leads to the formation of oxygen radicals, including the hydroxyl radical.[1] It is for this reason that iron levels are carefully controlled, normal individuals absorbing between 1 and 2 mg/24 h. This intake matches the daily loss of iron. In the extracellular compartment, iron is transferred between cells bound to the high-affinity iron-binding protein transferrin, whereas ferritin acts as a powerful iron buffer in intracellular compartments. Thus under normal physiological conditions only a vanishingly small amount of nonspecifically bound iron exists. However there are conditions where the iron status can change, for instance with idiopathic hemochromatosis[2] and transfusion-induced iron overload.[3] In such circumstances, either by virtue of hyperabsorption of iron from the intestine or by regular transfusion, iron overload results. Once transferrin and ferritin become saturated with iron, free radical-induced tissue damage results. Iron overload associated with transfusion-dependent β-thalassemia major results in irreversible damage to endocrine organs and lethal cardiac toxicity. In humans such excess iron cannot be excreted via the normal routes, namely, the urine and the bile, and consequently chelation therapy is essential.[3]

Ideally, administration of an iron-selective chelator should not interfere with iron-dependent enzymes and respiratory proteins, and the resulting complex should prevent the coordinated iron from redox cycling, thereby preventing the production of toxic free radicals.[4] Parenteral chelation therapy using desferrioxamine (DFO) is now well-established and this natural sidero-phore is capable of promoting negative iron balance and

---

reversing cardiac toxicity. Unfortunately, desferrioxamine (DFO) lacks oral activity, and this has a dramatic influence on patient compliance.[5]

There has been considerable interest in the design of orally active iron chelators over the past 20 years, and many high-affinity iron(III)-binding compounds have been prepared.[6-8] In principle it is possible to design hexadentate, tridentate, and bidentate ligands which are capable of providing a single iron(III) cation with the desired octahedral field. Bidentate and tridentate ligands have the advantage of low molecular weight, which favors efficient absorption from the gastrointestinal tract. In contrast, hexadentate ligands possess high molecular weights, typically falling in the range 350–1000, and consequently are less efficiently absorbed.[9] Hexadentate ligands which fall toward the lower end of this range belong to the amino carboxylate family, for instance HBED,[10] and these all possess an appreciable affinity for zinc(II).[4,11] In similar fashion the majority of iron(III)-binding tridentate ligands include nitrogen as one of the coordinating ligands; again this endows the molecule with appreciable affinity for zinc(II).[4,12] In contrast, it is possible to optimize the Fe(III)/Zn(II) selectivity using bidentate ligands, for instance, with substituted catechols[13,14] and 3-hydroxypyridin-4-ones (HPOs).[11]

The introduction of 3-hydroxypyridin-4-ones as iron-selective chelators has demonstrated that the design of orally active iron chelators is possible, but at the present time a compound with acceptable therapeutic potential has not been identified.[15] The long-term efficacy and toxicity of Deferiprone (L1 or CP20), 1,2-dimethyl-3-hydroxy-4(1*H*)-pyridinone, the first HPO to enter clinical trials, have yet to be established. One of the problems with such *N*-alkyl-3-hydroxypyridin-4-ones is the ability of the free ligand and the resulting iron complex to rapidly penetrate cell membranes and other biological barriers.[11] A second major difficulty is that *N*-alkyl-3-hydroxypyridin-4-ones are rapidly metabolized by glucuronidation of the 3-hydroxyl function (eq 1).[16] Such conjugation abolishes the iron-chelating

$$(1)$$
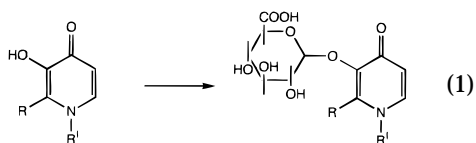
properties of the molecule. In principle both the difficulties could be minimized by using more hydrophilic hydroxypyridinones, the lower log D value leading to reduced membrane permeability and reduced susceptibility toward phase 2 conjugation reactions. However absorption by the gastrointestinal tract and the liver is also likely to be reduced with such compounds. Furthermore extremely hydrophilic chelators may become trapped intracellularly thereby inducing toxic side effects.[9] To investigate these possibilities we have extended the range of hydroxypyridinones reported previously, thus enabling us to investigate HPO–iron complexes with log D values spanning a range of 7 orders of magnitude. We report the relationship between the log D values of the free ligand and their iron-(III) complexes and the influence of distribution coeffi-

Scheme 1. Synthesis of 1-Alkyl-3-hydroxy-4(1*H*)-pyridinones
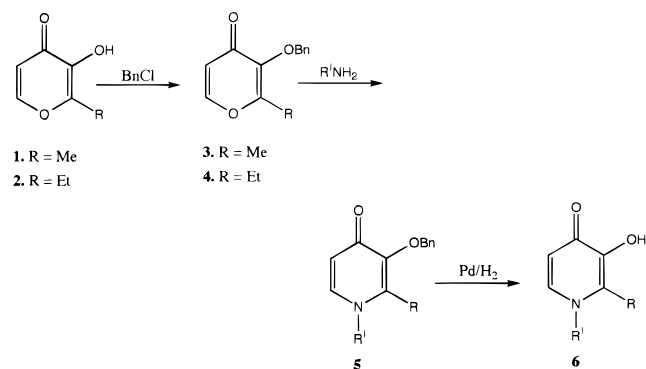
cient on the efficacy of selected HPOs in a cannulated bile duct rat model and a [^{59}Fe]ferritin-loaded rat model.

Chemistry

The 1-substituted-2-alkyl-3-hydroxy-4(1*H*)-pyridinones in this study were synthesized utilizing the methodology described by Dobbin and co-workers[17] (Scheme 1, Table 1). The commercially available 2-alkyl-3-hydroxy-4(1*H*)-pyranones maltol and ethylmaltol[18] were benzylated in 90% aqueous methanol to give **3** and **4**, respectively. Reactions of these adducts with primary amines were invariably performed under reflux in 50% aqueous ethanol in the presence of a catalytic amount of sodium hydroxide. 1-Amino-2-methyl-2-propanol is not commercially available and consequently was prepared via reduction of acetone cyanohydrin with LiAlH$_4$.[19] The reaction of benzylmaltol with serine in aqueous ethanol gave the expected benzylated product in the form of free base, but this compound being very hydrophilic was not extractable in organic solvents at pH 7. Thus the more hydrophobic amine 1,3-bis-(benzyloxy)-2-aminopropane was prepared from 1,3-bis-(benzyloxy)-2-propanol via a two-step reaction[20,21] and was subsequently reacted with benzylmaltol. The resulting protected HPO was found to partition from aqueous solution (pH 7) into dichloromethane and was finally purified by column chromatography. Where possible the benzylated pyridinones **5** were isolated in a crystalline form as either the free bases or the hydrochloride salts. Removal of the protecting benzyl group was achieved by catalytic hydrogenolysis invariably to yield the corresponding bidentate chelators **6** as either the free bases or the hydrochloride salts (Table 2).

The esters **65** and **66** were synthesized by treating the benzylated carboxylic acid derivatives with the corresponding alcohol in the presence of triphenylphosphine and diethyl azodicarboxylate.[22] The amide analogues **69** and **76–79** were obtained via reaction of the succinimidyl-activated ester **7a** with primary amines in two steps or the in situ formation of the benzotriazolyl-activated ester **7c** (Scheme 2) in one step in the presence of 2-(1*H*-benzotriazol-1-yl)-1,1,3,3-tetramethyluronium tetrafluoroborate (TBTU) as an activating agent[23,24] (Table 2).

Determination of Solution Properties

3-Hydroxy-4(1*H*)-pyridinones possess two pK_a values, one corresponding to the 4-oxo function (p$K_a \approx 3.7$) and the second corresponding to the 3-hydroxyl function (pK_a

Table 1. 1-Substituted-2-alkyl-3-(benzyloxy)- and -3-hydroxy-4(1H)-pyridinones (Bn = benzyl)
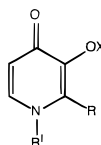
compd	R′	R	X	ref
8	CH$_2$C(CH$_3$)$_2$OH	Me	Bn	
9	CH(CH$_2$OBn)$_2$	Me	Bn	
10	CH$_2$CH$_2$CH$_2$OH	Et	Bn	
11	CH$_2$CH$_2$CH$_2$CH$_2$OH	Et	Bn	
12	CH$_2$CH(OMe)$_2$	Me	Bn	
13	CH$_2$CH(OEt)$_2$	Me	Bn	
14	CH$_2$CH$_2$COOH	Et	Bn	
15	CH$_2$CH$_2$CH$_2$COOH	Et	Bn	
16	CH$_2$CH$_2$COOH	Me	Bn	17
17	CH$_2$CH$_2$CH$_2$COOH	Me	Bn	17
18	CH$_2$CH$_2$SO$_3$H	Me	Bn	
19	CH$_2$CH$_2$COOCH$_3$	Me	Bn	
20	CH$_2$CH$_2$COOCH$_2$CH$_3$	Me	Bn	
21	CH$_2$CH$_2$CH$_2$CONHMe	Me	Bn	
22	CH$_2$CH$_2$CONHMe	Et	Bn	
23	CH$_2$CH$_2$CONHPr	Et	Bn	
24	CH$_2$CH$_2$CON(Me)$_2$	Et	Bn	
25	CH$_2$CH$_2$CON(Et)$_2$	Et	Bn	
26	H	Me	H	17, 46
27	Me	Me	H	17, 46
28	Et	Me	H	17, 45
29	CH$_2$CH=CH$_2$	Me	H	45
30	CH$_2$CH$_2$CH$_3$	Me	H	17, 45
31	CH$_2$CH$_2$CH$_2$CH$_3$	Me	H	17
32	CH(CH$_3$)$_2$	Me	H	17
33	CH$_2$CH(CH$_3$)$_2$	Me	H	17
34	CH$_2$CH$_2$CH$_2$CH$_2$CH$_3$	Me	H	17
35	CH$_2$CH$_2$CH$_2$CH$_2$CH$_2$CH$_3$	Me	H	17
36	C$_6$H$_5$	Me	H	17, 47
37	H	Et	H	17
38	Me	Et	H	17, 45
39	Et	Et	H	17, 45
40	CH$_2$CH=CH$_2$	Et	H	45
41	CH$_2$CH$_2$CH$_3$	Et	H	17
42	CH(CH$_3$)$_2$	Et	H	17
43	CH$_2$CH$_2$CH$_2$CH$_3$	Et	H	17
44	CH$_2$CH$_2$OH	Me	H	17
45	CH$_2$CH$_2$CH$_2$OH	Me	H	17
46	CH$_2$CH$_2$CH$_2$CH$_2$OH	Me	H	17
47	CH$_2$C(CH$_3$)$_2$OH	Me	H	
48	CH$_2$CH(OH)CH$_2$OH	Me	H	
49	CH(CH$_2$OH)$_2$	Me	H	
50	CH$_2$CH$_2$OH	Et	H	17
51	CH$_2$CH$_2$CH$_2$OH	Et	H	
52	CH$_2$CH$_2$CH$_2$CH$_2$OH	Et	H	
53	CH$_2$CH$_2$OMe	Me	H	17
54	CH(CH$_3$)CH$_2$OMe	Me	H	17
55	(CH$_2$)$_3$OEt	Me	H	17
56	CH$_2$CH(OMe)$_2$	Me	H	
57	CH$_2$CH(OEt)$_2$	Me	H	
58	CH$_2$CH$_2$OMe	Et	H	17
59	(CH$_2$)$_3$OEt	Et	H	17
60	CH$_2$CH$_2$COOH	Me	H	17
61	CH$_2$CH$_2$CH$_2$COOH	Me	H	17
62	CH$_2$CH$_2$COOH	Et	H	
63	CH$_2$CH$_2$CH$_2$COOH	Et	H	
64	CH$_2$CH$_2$SO$_3$H	Me	H	
65	CH$_2$CH$_2$COOMe	Me	H	
66	CH$_2$CH$_2$COOEt	Me	H	
67	CH$_2$CH$_2$NH$_2$	Me	H	17
68	(CH$_2$)$_2$CONHMe	Me	H	17
69	(CH$_2$)$_3$CONHMe	Me	H	
70	(CH$_2$)$_2$CONHEt	Me	H	17
71	(CH$_2$)$_2$CONHPr	Me	H	17
72	(CH$_2$)$_2$CONHiPr	Me	H	17
73	(CH$_2$)$_2$CONMeEt	Me	H	17
74	(CH$_2$)$_2$CON(Me)$_2$	Me	H	17
75	CH$_2$CH$_2$CON(Et)$_2$	Me	H	17
76	(CH$_2$)$_2$CONHMe	Et	H	
77	(CH$_2$)$_2$CONHPr	Et	H	
78	(CH$_2$)$_2$CON(Me)$_2$	Et	H	
79	(CH$_2$)$_2$CON(Et)$_2$	Et	H	

$\approx$ 9.8).[17] These bidentate ligands also form a number of complexes with iron(III) so that aqueous solutions equilibrate to give mixtures in which the speciation depends on the metal ion, ligand, and hydrogen ion concentrations. A simple model of this system is shown in equation (eq 2). This model has previously been

$$Fe^{3+} + L^- \rightleftharpoons FeL^{2+} \quad (K_1)$$

$$FeL^{2+} + L^- \rightleftharpoons FeL_2^+ \quad (K_2) \qquad (2)$$

$$FeL_2^+ + L^- \rightleftharpoons FeL_3 \quad (K_3)$$
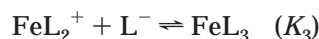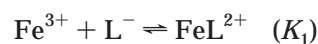
shown to apply to 3-hydroxy-4(1H)-pyridinones.[25] Both the pK_a values and stability constants were obtained by global optimization of parameters corresponding to titrations at several different ligand and iron(III) concentrations. The experimental conditions ensured that the most associated species predominated.

Distribution coefficients (*D* values) of the 3-hydroxy-4(1H)-pyridinones and the iron(III) complexes were determined in an aqueous/octanol system using a filter probe device.[17,26] However, reproducible values for extremely hydrophobic compounds (log *D* values > 2) or hydrophilic compounds (log *D* < −2) were difficult to obtain using the filter probe. The distribution coefficients for such compounds were determined by the "shake-flask" method changing the ratio of the two phases (aqueous/1-octanol) to, for instance, 100:1 for hydrophobic compounds (log *D* values > 2) and 1:100 for hydrophilic compounds (log *D* < −2), respectively.[27]

Biological Experiments

A selection of hydroxyalkyl-substituted hydroxypyridinones were tested for their ability to remove iron from non-iron-overloaded rats. The bile duct was cannulated, and the quantity of iron excreted by the bile in the presence and absence of chelators was determined and expressed as μg of Fe/kg of animal weight.[28] In a parallel study chelators were also investigated in a [59-Fe]ferritin-loaded rat model.[29] Ferritin, which has a molecular weight of approximately 450 000, is one of the major iron storage proteins in the body. It consists of 24 equivalent subunits which provide a hollow center capable of accommodating up to 4000 iron atoms in the form of a regular ferric−hydroxide−phosphate lattice. Since ^{59}Fe-labeled ferritin is predominantly taken up by hepatocytes in rats, it can be used to label the liver iron pool selectively.[30] Thus this [59Fe]ferritin-loaded rat model can be used to compare the ability of chelators to remove iron from the liver, the major storage organ in iron-overloaded conditions.

Results

Distribution Coefficients. The distribution coefficients (log *D*) of the free ligands and their iron(III) complexes between an aqueous phase buffered at pH 7.4 and octanol are presented in Table 3. In general, as expected the increase in the length of the alkyl chain on the heterocyclic nitrogen results in an increase in the log *D* values of both the ligand and the iron(III) complex. In most cases iron(III) complexes are more hydrophilic than their corresponding free ligands. However, this trend did not hold for those compounds which

Table 2. Synthesis of 1-Substituted-2-alkyl-3-hydroxy-4(1H)-pyridinones Isolated as Free Bases or Hydrochloride Salts

compd	R	R′	mp, °C	% yield	formula	anal.
47	Me	$CH_2C(CH_3)_2OH$	204−205	80	$C_{10}H_{15}NO_3$	CHN
49	Me	$CH(CH_2OH)_2$	225−226	71	$C_{19}H_{14}NO_4Cl$	CHNCl
51	Et	$CH_2CH_2CH_2OH$	147−148	96	$C_{10}H_{16}NO_3Cl$	CHNCl
52	Et	$CH_2CH_2CH_2CH_2OH$	166−167	98	$C_{11}H_{18}NO_3Cl$	CHNCl
56	Me	$CH_2CH(OMe)_2$	213−214	78	$C_{10}H_{15}NO_4$	CHN
57	Me	$CH_2CH(OEt)_2$	116−117	80	$C_{12}H_{19}NO_4$	CHN
62	Et	CH_2CH_2COOH	167−168	87	$C_{10}H_{13}NO_4$	CHN
63	Et	$CH_2CH_2CH_2COOH$	190−191	64	$C_{11}H_{15}NO_4$	CHN
64	Me	$CH_2CH_2SO_3H$	>300	85	$C_8H_{11}NO_5S$	CHNS
65	Me	CH_2CH_2COOMe	142−144	85	$C_{10}H_{14}NO_4Cl$	CHNCl
66	Me	CH_2CH_2COOEt	149−151	90	$C_{11}H_{16}NO_4Cl$	CHNCl
69	Me	$CH_2CH_2CH_2CONHMe$	207−209	95	$C_{11}H_{17}N_2O_3Cl$	CHNCl
76	Et	$CH_2CH_2CONHMe$	165−166	96	$C_{11}H_{17}N_2O_3Cl$	CHNCl
77	Et	$CH_2CH_2CONHPr$	157−158	95	$C_{13}H_{21}N_2O_3Cl$	CHNCl
78	Et	$CH_2CH_2CONMe_2$	136−137	86	$C_{12}H_{19}N_2O_3Cl$	CHNCl
79	Et	$CH_2CH_2CONEt_2$	153−154	85	$C_{14}H_{23}N_2O_3Cl$	CHNCl

Scheme 2. Synthesis of 1-[(*N*-Alkylcarbamoyl)alkyl]-2-alkyl-3-hydroxy-4(1H)-pyridinone
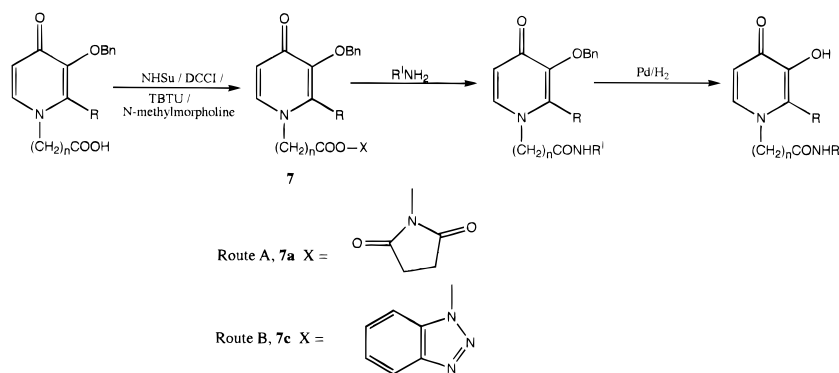
have log D values greater than 3 (i.e., **31**, **33**−**36**, **41**−**43**, and **59**). In these examples the iron(III) complexes were found to be more hydrophobic than their corresponding free ligands. Surprisingly, the unsubstituted pyridinones **26** and **37** possess higher values than the *N*-methylpyridinones **27** and **38**. This trend also holds for the corresponding iron(III) complexes. The charged molecules **60**−**63** and **67** possess the lowest values. Among the neutral compounds, **35** and **49** possess the highest and the lowest log D values, respectively, and not surprisingly they form the most hydrophobic and hydrophilic iron(III) complexes, respectively.

A plot of the log D values of the neutral ligands against the log D values of the corresponding iron(III) complexes demonstrates the existence of a biphasic linear relationship between the log D values of ligand and complex (Figure 1). A simple equation (eq 3) was derived relating these two parameters for ligands with log $D_{ligand} = -1$. The more hydrophilic ligands (log $D_{ligand} < -1$) possess a different relationship yielding the corresponding equation (eq 4). The entire range of log D_{ligand} values of the ligands covers 3 orders of magnitude, whereas for the corresponding iron(III) complexes, this range spans 7 orders of magnitude.

$$\log D_{ligand} = 2.53 \log D_{complex} - 0.80 \quad (r = 0.99) \quad (3)$$

$$\log D_{ligand} = 0.49 \log D_{complex} - 2.45 \quad (r = 0.99) \quad (4)$$

Ligand pK_a Values. Some representative ligands, the hydroxyalkyl derivatives (**44** and **50**) and the carboxyalkyl derivatives (**60**, **62**, and **63**), have been studied by simultaneous spectrophotometric/potentiometric titrations. The (hydroxyalkyl)pyridinones possess two pK_a values, pK_{a1} and pK_{a2}, whereas the (carboxyalkyl)pyridinones possess three, pK_{a1}, pK_{a2}, and pK_{a3}. For the (hydroxyalkyl)pyridinones, pK_{a1} is associated with the protonation of the 4-oxo group and pK_{a2}, the protonation of the 3-hydroxy function (Scheme 3). The pK_{a2} value of the (carboxyalkyl)pyridinone corresponds to the carboxylic function and can be distinguished from the similar value of pK_{a1} by the absence of a spectrophotometric change. The optimized pK_a values obtained with NONLIN15[25] are shown in Table 4. The values were found to be relatively constant irrespective of the N-substituent.

Speciation plots relating to these values are presented in Figure 2. The neutral form of the (hydroxyalkyl)-pyridinones, as typified by **50**, dominates the plot over the pH range 4−9, whereas the neutral form of the (carboxyalkyl)pyridinones, as typified by **62**, only makes a minor contribution, the monoanion dominating over the pH range 5−9.

Stability Constants of Iron(III) Complexes. For pyridinones **50** and **62**, the K_1, K_2, and K_3 values were determined and compared with the corresponding β_3 values, the latter resulting from competitive titration

Table 3. log Distribution Coefficient (log D) Values of Ligands and Fe Complexes (n = no. of replications)

compd	R′	R	log D ligand	n	log D Fe complex	n
26	H	Me	-0.50 ± 0.02	5	-2.38 ± 0.02^a	4
27	Me	Me	-0.77 ± 0.02	6	-2.60 ± 0.05^a	4
28	Et	Me	-0.31 ± 0.01	5	-1.59 ± 0.08	6
29	CH$_2$CH=CH$_2$	Me	0.03 ± 0.01	5	-0.70 ± 0.02	6
30	Pr	Me	0.18 ± 0.01	10	-0.08 ± 0.01	6
31	(CH$_2$)$_3$CH$_3$	Me	0.70 ± 0.01	10	1.36 ± 0.03	6
32	CH(CH$_3$)$_2$	Me	0.05 ± 0.01	5	-0.54 ± 0.03	5
33	CH$_2$CH(CH$_3$)$_2$	Me	0.65 ± 0.02	5	1.26 ± 0.02	6
34	(CH$_2$)$_4$CH$_3$	Me	1.24 ± 0.01	10	2.74 ± 0.02^a	4
35	(CH$_2$)$_5$CH$_3$	Me	1.89 ± 0.02	6	3.40 ± 0.02^a	4
36	C$_6$H$_5$	Me	1.01 ± 0.01	6	2.16 ± 0.02	4
37	H	Et	0.05 ± 0.01	8	-1.16 ± 0.01	6
38	Me	Et	-0.21 ± 0.01	5	-1.50 ± 0.02	6
39	Et	Et	0.23 ± 0.01	10	-0.62 ± 0.02	10
40	CH$_2$CH=CH$_2$	Et	0.47 ± 0.01	5	0.36 ± 0.01	8
41	Pr	Et	0.70 ± 0.01	6	0.96 ± 0.01	8
42	CH(CH$_3$)$_2$	Et	0.73 ± 0.01	5	1.01 ± 0.01	5
43	(CH$_2$)$_3$CH$_3$	Et	1.22 ± 0.01	10	2.36 ± 0.02^a	4
44	CH$_2$CH$_2$OH	Me	-1.10 ± 0.01	5	-3.00 ± 0.08^a	4
45	CH$_2$CH$_2$CH$_2$OH	Me	-0.89 ± 0.01	5	-2.92 ± 0.07^a	4
46	(CH$_2$)$_4$OH	Me	-0.75 ± 0.01	7	-2.75 ± 0.05^a	4
47	CH$_2$C(CH$_3$)$_2$OH	Me	-0.77 ± 0.02	5	-2.33 ± 0.04^a	4
49	CH(CH$_2$OH)$_2$	Me	-1.70 ± 0.04	4	-3.30 ± 0.04^a	4
50	CH$_2$CH$_2$OH	Et	-0.66 ± 0.02	5	-2.75 ± 0.07^a	4
51	CH$_2$CH$_2$CH$_2$OH	Et	-0.32 ± 0.01	5	-2.10 ± 0.01^a	4
52	(CH$_2$)$_4$OH	Et	-0.28 ± 0.01	5	-1.68 ± 0.02	5
53	CH$_2$CH$_2$OMe	Me	-0.41 ± 0.01	5	-1.85 ± 0.05	5
54	CH(CH$_3$)CH$_2$OMe	Me	-0.26 ± 0.01	5	-1.40 ± 0.03	5
55	(CH$_2$)$_3$OEt	Me	0.12 ± 0.01	5	-0.52 ± 0.04	5
56	CH$_2$CH(OMe)$_2$	Me	-0.46 ± 0.03	5	-2.52 ± 0.06^a	4
57	CH$_2$CH(OEt)$_2$	Me	0.21 ± 0.01	6	-0.10 ± 0.02	10
58	CH$_2$CH$_2$OMe	Et	0.04 ± 0.01	5	-1.16 ± 0.03	5
59	(CH$_2$)$_3$OEt	Et	0.72 ± 0.01	5	0.99 ± 0.01	6
60	CH$_2$CH$_2$CO$_2$H	Me	-2.92 ± 0.07^a	4	-4.00 ± 0.15^a	4
61	CH$_2$CH$_2$CH$_2$CO$_2$H	Me	-2.75 ± 0.07^a	4	-3.70 ± 0.06^a	5
62	CH$_2$CH$_2$CO$_2$H	Et	-1.60 ± 0.01	5	-3.22 ± 0.03^a	5
63	CH$_2$CH$_2$CH$_2$CO$_2$H	Et	-1.38 ± 0.01	5	-3.10 ± 0.03^a	4
65	CH$_2$CH$_2$CO$_2$Me	Me	-0.77 ± 0.02	8	-2.70 ± 0.04^a	4
66	CH$_2$CH$_2$CO$_2$Et	Me	-0.24 ± 0.01	5	-1.16 ± 0.01	6
67	CH$_2$CH$_2$NH$_2$	Me	-1.55 ± 0.01	5	-3.22 ± 0.03	4
68	(CH$_2$)$_2$NHCOMe	Me	-1.15 ± 0.01	5	-3.05 ± 0.03^a	4
69	(CH$_2$)$_3$CONHMe	Me	-1.08 ± 0.01	8	-3.00 ± 0.11^a	4
70	(CH$_2$)$_2$CONHEt	Me	-0.82 ± 0.02	5	-2.70 ± 0.06^a	4
71	(CH$_2$)$_2$CONHPr	Me	-0.40 ± 0.01	5	-1.52 ± 0.01	5
72	(CH$_2$)$_2$CONHiPr	Me	-0.47 ± 0.01	5	-1.89 ± 0.07	5
73	(CH$_2$)$_2$CONMeEt	Me	-0.66 ± 0.02	5	-2.52 ± 0.04^a	4
74	(CH$_2$)$_2$CON(Me)$_2$	Me	-1.00 ± 0.01	5	-3.00 ± 0.11^a	4
75	CH$_2$CH$_2$CONEt$_2$	Me	-0.36 ± 0.01	5	-1.70 ± 0.02	5

^{a} Determination by hand-shake method. Determinations made for 1-octanol/water (pH 7.4) system at 25 °C.

with EDTA. The optimized values are presented in Table 4, where it can be seen that there is excellent agreement between the summation of log K_1, K_2, and K_3 values with the directly determined log β_3 value for compounds **50** and **62**. The pH titration curve for pyridinone **50** in the presence of iron(III) is displayed in Figure 3: at low pH values the λ_{max} of the iron(III) complex (545 nm) corresponds to the Fe^{III}L$_1^{2+}$ complex; over the pH range 3.5–5.5, the Fe^{III}L^{2+} complex (λ_{max}, 510 nm) dominates; and above pH 7.0 the neutral Fe^{III}L$_3$ complex (λ_{max}, 460 nm) dominates.

The β_3 values are not markedly influenced by the net charge of the FeL$_3$ complex, which is neutral for **50**, and 3^- for **62**. Although the value of log K_1 is predictably larger for the charged pyridinone **62**, this is balanced
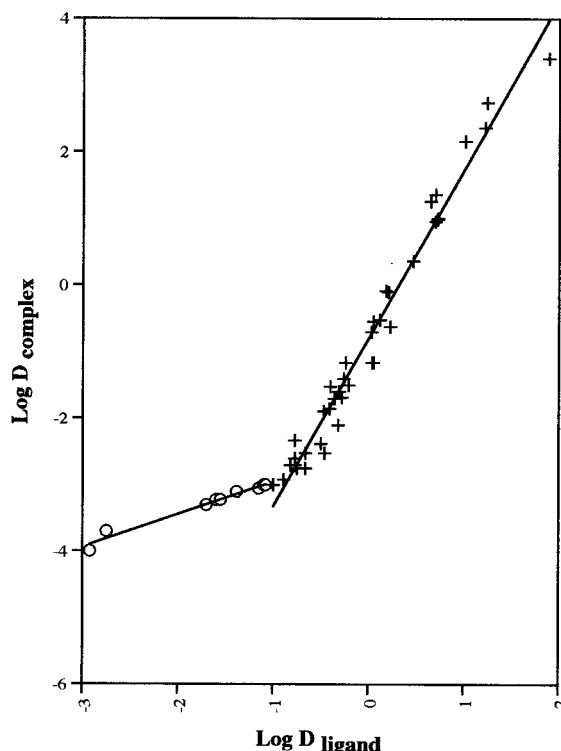
Figure 1. Relationship between the log D value of Fe complex (log $D_{complex}$) and log D value of hydroxypyridinone (log D_{ligand}). Distribution coefficients were determined using a MOPS buffer (50 mM, pH 7.4)/octanol system.

Scheme 3
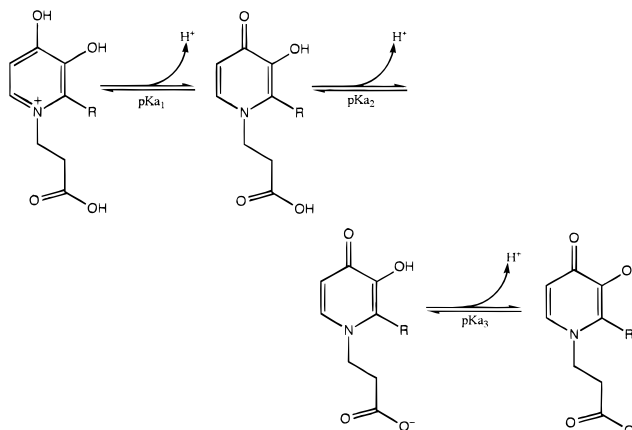
by a proportionate decrease in the value of log K_3 (Table 4). Thus the log β_3 value remains remarkably constant. Indeed log β_3 values for **26**, **28**, **30**,[17] **39**,[31] and **50** (Khodr and Hider, unpublished) all fall within the range 36.8–37.7. For this reason we did not determine the β_3 values of the entire set of the ligands. The speciation plot for pyridinone **62** in the presence of iron(III) (Figure 4) indicates that the FeL$_3$ complex dominates over the pH range 6.5–10. An energy-minimized structure of the iron(III) complex of **50** using Hyperchem Software (Molecular Modeling, release II for SGI) is presented in Figure 5.

Ability of 3-Hydroxypyridinones To Facilitate the Excretion of Iron in Bile. The 3-hydroxypyridin-4-one Deferiprone (**27**) is orally active in this rat test system, although as demonstrated in humans less effective than desferrioxamine when administered pa-

Table 4. Spectrophotometric and Potentiometric Determined pK_a Values for Ligands and Affinity Constants for Fe(III) Complexes

| | pK_{a1} | | | pK_{a2}/pK_{a3} [a] | | affinity constants for Fe(III) | | | log β_3 | |
| | | | | | | | | | | |
ligand	potentio-metric	spectrophoto-metric	pK_{a2}	potentio-metric	spectrophoto-metric	log K_1	log K_2	log K_3	summation K_1, K_2, K_3	EDTA competition value
27		3.56			9.64	14.9	12.2	9.8	37.2	
44	3.44	3.43		9.65	9.72					
50	3.31	3.34		9.77	9.75	15.7	11.6	9.4	36.7	36.8
60	3.10	3.19	3.79	9.49	9.51					
62	3.12	3.22	3.91	9.89	9.91	16.6	11.4	7.9	36.9	37.0
63	3.21	3.42	4.27	9.89	9.99					

[a] pK_{a2} for **27**, **44**, and **50**; pK_{a3} for **60**, **62**, and **63**.

Figure 3. pH dependence of the spectrum of ligand **50** in the presence of Fe(III). [Fe(III)] = 1.889 × 10^{-4} M, [**50**] = 1.901 × 10^{-3} M. The isosbestic point at 510 nm corresponds to the conversion of the 2:1 complex to the 3:1 complex.
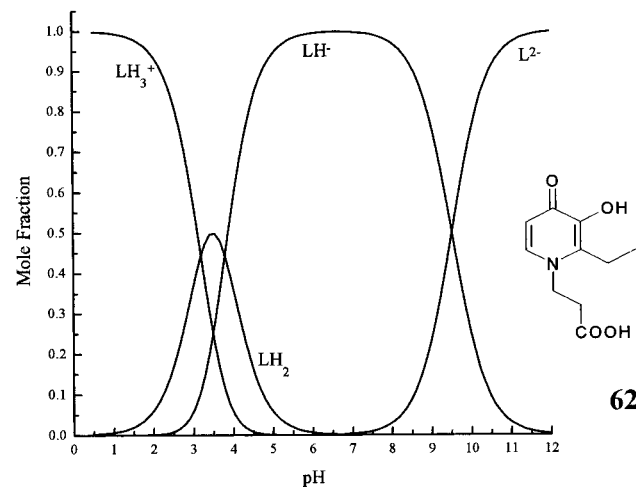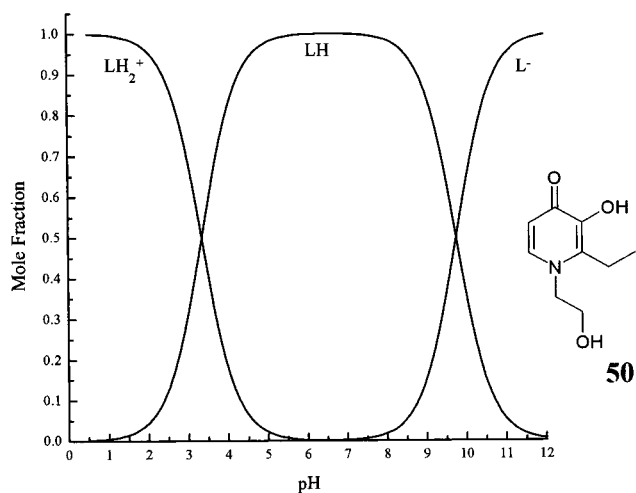
Figure 2. Speciation plots of hydroxypyridinones **50** and **62**. The following parameters were incorporated into the model for the system: for **50**, pK_{a1} = 3.34, pK_{a2} = 9.75; **62**, pK_{a1} = 3.22, pK_{a2} = 3.91, pK_{a3} = 9.91.
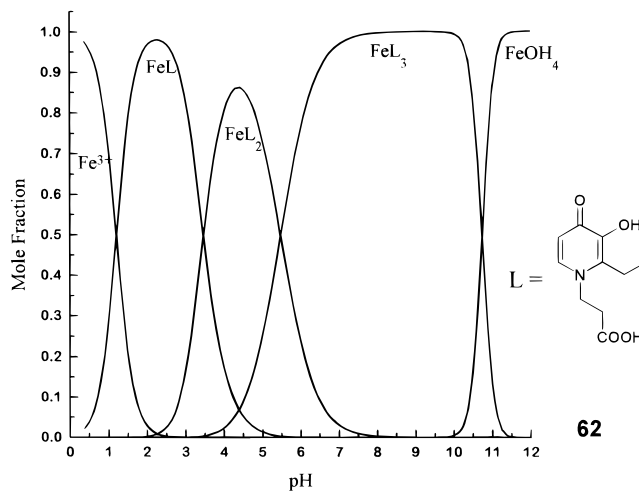
Figure 4. Speciation plot of **62** (5 × 10^{-5} M) in the presence of iron(III) (1 × 10^{-5} M). The following parameters were incorporated into the model for the system: log β_1ML = 16.61, log β_2ML$_2$ = 28.05, log β_3ML$_3$ = 36.93, pK_{a1} = 3.22, pK_{a2} = 3.91, pK_{a3} = 9.91, pK(FeOH) = −3.03, pK((FeOH)$_2$) = −6.30, and pK((FeOH)$_3$) = −2.9.

rentally (Table 5). Similar profiles were observed for the pyridinones **45** and **51**, both of which had similar efficacies to that of **27** (Figure 6). The extremely hydrophilic pyridinone **48** possessed an extremely low activity. In contrast, the 1-(2′-hydroxyethyl)pyridinones (**44** and **50**) induced more prolonged periods of iron excretion, and compound **50** was found to be markedly more active than both Deferiprone (**27**) and desferrioxamine in this test system (Table 5, Figure 6).

Ability of 3-Hydroxypyridinones To Facilitate the Excretion of ^{59}Fe from Ferritin-Loaded Rats. Rats were infused with ^{59}Fe-rat ferritin (10 μg), and after a 1-h period the pyridinones were administered

by oral gavage. During this period the [^{59}Fe]ferritin is efficiently cleared from the systemic circulation by the hepatocytes where it is catabolized and incorporated into endogenous ferritin via the cytoplasm labile iron pool. It is likely that the orally administered chelators scavenge iron from this pool. Again the hydroxyl-substituted-*N*-alkylpyridinones were demonstrated to be
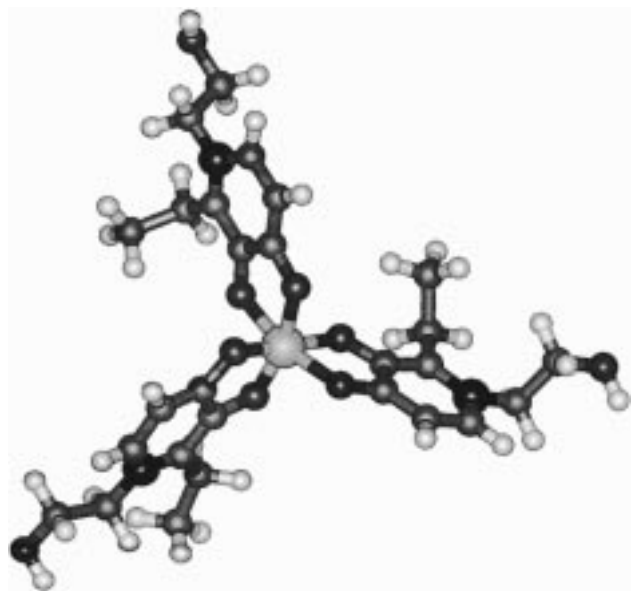
Figure 5. Energy-minimized structure of the iron(III) complex of **50**: white, hydrogen; gray, carbon; black, oxygen and nitrogen.

Table 5. Influence of Chelators on Iron Excretion in the Bile Duct-Cannulated Rats[a]

	dose		iron excretion, $\mu g\ kg^{-1}$	
compd	mg kg^{-1}	iron-binding equivalent in mequiv kg^{-1}	oral	subcutaneous
27	100	0.24	351 ± 38	292 ± 35
DFO	100	0.15		527 ± 131
44	122	0.24	272 ± 100	353 ± 61
45	132	0.24	414 ± 44	383 ± 33
48	143	0.24	104 ± 75	142 ± 50
50	132	0.24	819 ± 22	698 ± 58
51	142	0.24	265 ± 153	634 ± 266

[a] The results are the mean ± SD iron excreted in bile and urine from 3−4 animals.

orally active in this test system, although only **45** was found to be significantly better than Deferiprone (**27**) (Figure 7). The carboxylate-containing hydroxypyridinone **60** was found to be equieffective as **27**, but none of these relatively hydrophilic chelators were as effective as the more lipophilic pyridinone **39**.

Discussion

Fifty-four 3-hydroxypyridin-4-ones have been synthesized covering a wide range of distribution coefficients. All bind iron(III) tightly to form neutral 3:1 complexes over the pH range 5−9.5. The relationship between the noncharged ligand D values (D_{ligand}) and the corresponding D values of the iron complexes ($D_{complex}$) for ligands with a log $D_{ligand} = -1$ is linear with a r value of 0.99 (Figure 1, eq 3). The more hydrophilic ligands (log $D_{ligand} < -1$) gave a different relationship (Figure 1, eq 4). In principle log D_{ligand} and log $D_{complex}$ will be an additive function of the varying contribution of the R and R′ groups. The electrically neutral iron(III) complex has three bidentate chelating molecules octahedrally coordinated to iron(III)[17,32] (Figure 5) so that it will have approximately 3 times the surface area of the ligand alone, the contribution of the iron atom being negligible[33,34] as it is completely coordinated by the six coordinating ligands. Consequently it might be ex-
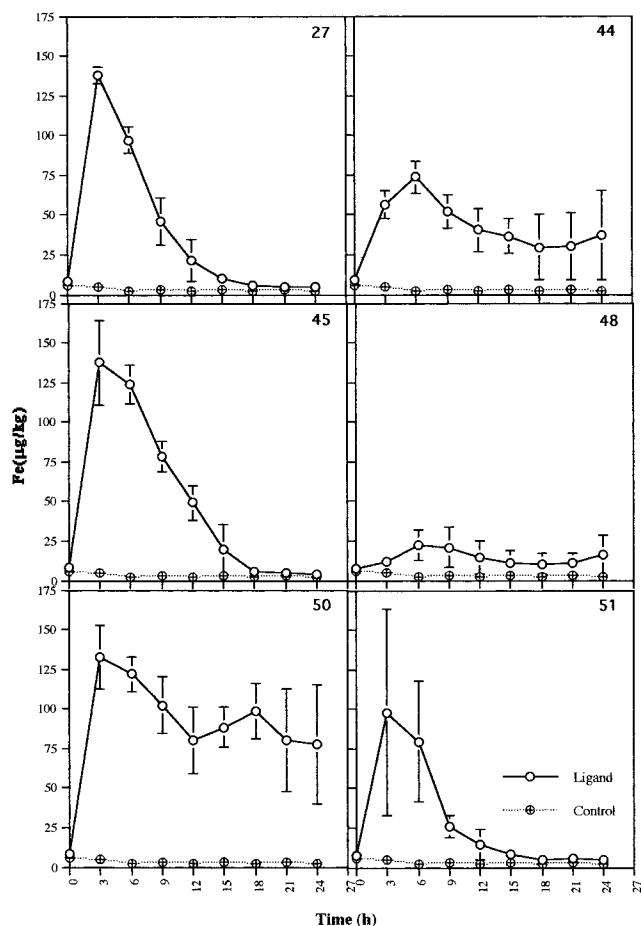
Figure 6. Hydroxypyridinone-induced iron excretion by the rat bile duct. The chelators **27**, **44**, **45**, **48**, **50**, and **51** were given orally. Chelator dose was 450 μmol/kg ($n = 3$).
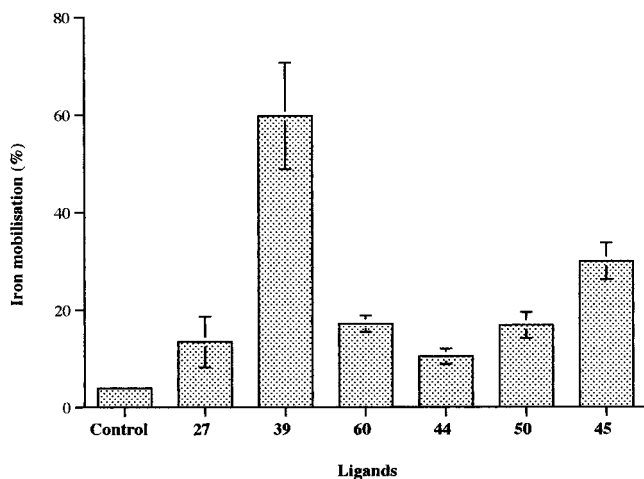
Figure 7. Biliary ^{59}Fe excretion induced by hydroxypyridinones from ferritin-loaded rats. The chelators **27**, **39**, **44**, **45**, **50**, and **60** were given orally. Chelator dose was 450 μmol/kg ($n = 5-9$).

pected that a relationship similar to eq 3 would result[34] where k is a constant representing the change in hydrophobicity in converting the six hydrophilic ligating groups of the three hydroxypyridinones into the coordinating sphere of the iron(III) complex. The effective masking (or partial masking) of the oxygen atoms on the 3- and 4-positions of the hydroxypyridinone ring on complexation leads to an increase in the lipophilicity

contribution of the complex, and this difference should be constant irrespective of the nature of the substitution R and R′. This constant difference is represented by the negative constant −0.80 in eq 3. The slope of 2.53 is appreciably smaller than the theoretical slope of 3.00, and this probably represents the relatively efficient packing of the three ligands in the iron(III) complex; i.e., the surface area is <3 times that of the free ligand. Significantly Edward et al.[34] observed a similar effect in a parallel study centered on the chelation of iron(III) by pyridoxal hydrazones, which are trident ligands. The observed slope was 1.94 as compared to the theoretical value of 2.0 and $k = -0.83$ ($r = 0.92$). In the same study these authors also included a limited range of hydroxypyridinones and obtained slightly different values of slope and k to those reported in this study. However some of the D values adopted in the earlier study have since been modified. It is not always convenient to measure the log $D_{complex}$ directly as the filter probe system can easily become contaminated with iron (Dobbin et al.[17] and this work). The relationships depicted in Figure 1 render it possible to make a reliable estimation of log $D_{complex}$ for a directly determined log D_{ligand}.

With the more hydrophilic hydroxypyridinones (log $D_{ligand} < -1$) (**44**, **49**, **60**–**63**, **67**–**69**), a deviation from eq 3 results with the log $D_{complex}$ values leveling out (Figure 1). The reason for this deviation is not clear but would indicate that the solvation in the aqueous phase is similar for both the free ligand and the complex for the more hydrophilic molecules and that therefore the difference between the log $D_{complex}$ and log D_{ligand} is less marked with this group of molecules.

When extremely hydrophilic pyridinones enter a cell, albeit slowly, and scavenge iron(III), the complex is predicted to efflux even more slowly due to its higher molecular weight and more hydrophilic nature. In principle this could lead to toxic side effects resulting from trapped intracellular iron. Furthermore as the systemic concentration of the hydroxypyridinone decreases, leading to a net pyridinone efflux, the 3:1 complex would be predicted to partially dissociate forming the charged 2:1 complex which would possess an even lower log D, by virtue of its net charge (eq 5).

$$H^+ + [Fe(HPO)_3]^0 \rightleftharpoons [Fe(HPO)_2]^+ + HPO^0 \quad (5)$$

The presence of such partially coordinated iron complexes may generate hydroxyl radicals.[1] Thus although (hydroxyalkyl)pyridinones possess the advantage of slow phase II metabolism, for instance glucuronidation (eq 1), and thereby retain iron-scavenging properties,[35] they may lead to the retention of iron by cells. However the flattening of the relationship between log $D_{complex}$ and log D_{ligand} with increasing hydrophilicity of the ligand will tend to minimize the effect.

One method of avoiding the above difficulty is to design hydroxypyridinones which are so hydrophilic that they are effectively unable to enter cells via passive diffusion. This is probably one of the reasons that desferrioxamine is relatively nontoxic.[36] In principle anionic hydroxypyridinones, by virtue of their hydrophilicity, could function in a similar manner. Speciation plots of carboxylate-containing hydroxypyridinones show

that the dominate species over the pH range 5.0−9.0 (Figure 2) is the monoanionic form (Scheme 3), and although the corresponding 3:1 iron(III) complex will possess a net charge close to 3− at pH 7.4, this complex dominates the speciation plot above pH 7.0 (Figure 4). As indicated in Figure 1, the ratio of log $D_{complex}$/log D_{ligand} for HPOs possessing a log D_{ligand} value > −0.1 is much lower than for neutral ligands, and thus the rate of efflux of 3:1 iron complexes is predicted not to markedly decrease with decreasing log D_{ligand} value. Thus this preliminary analysis and search for nontoxic hydroxypyridinones favors compounds with a log D_{ligand} value falling in the range −1 to −2. Hydroxypyridinones possessing a carboxylate function on the ring nitrogen substituent, for instance **60**−**63**, fall into this range (Table 3).

Two animal models were selected to monitor the ability of iron chelators to mobilize iron under in vivo conditions: the bile duct cannulated rat and the [59Fe]-ferritin-labeled rat. Both have a proven record for successfully identifying potentially useful iron chelators. Both models are designed to maintain the removal of iron from the hepatocyte, the liver being the major target organ in transfused β-thalassemia patients.[3] With the [59Fe]ferritin model, the labeled ferritin is rapidly removed from the circulation by hepatocytes, which then degrade the exogenous ferritin to iron which subsequently enters the so-called "labile iron pool". It is this pool of iron which is the specific target of orally active iron chelators. Unfortunately when administered orally, the carboxylate-containing hydroxypyridinone was found not to be highly efficient at extracting iron (Figure 7). Although Molenda and co-workers[37] reported oral activity for 6-carboxyl-3-hydroxy-1-methylpyridin-4-one (**80**),

80
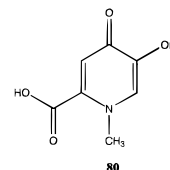
the compound was found to be more effective when given intravenously (80% of activity of Deferiprone, **27**) than when administered orally (38% activity of Deferiprone, **27**). In the present study a similar finding was made with **60** which is equiefficient with **27** (Figure 7). The difference between **60** and **80** will largely result from the higher D_{ligand} value of the former. Thus although monoanionic pyridinones are likely to be less toxic than Deferiprone (**27**), they are unlikely to be more efficient at scavenging iron, and the general opinion is that a ligand possessing a higher efficacy than Deferiprone (L1 or CP20) is required.[15] Similar arguments could be made for monobasic pyridinones, for instance **67**, although there is a greater possibility of such molecules inhibiting critical enzymes such as tyrosine hydroxylase.[38] Some (hydroxyalkyl)hydroxypyridinones are rapidly and efficiently metabolized to the corresponding monoanionic derivatives (eq 6)[35] and thus can be considered as prodrugs of the latter class of pyridinones. Such (hydroxyalkyl)pyridinones are also capable of facilitating the excretion of iron when administered orally (Figures 6 and 7). However the finding that **45** and **51** have similar activities to that of **27** (Deferiprone)
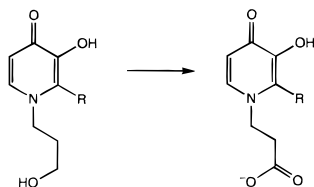
indicates that such a metabolic change does not offer an advantage over Deferiprone (**27**) in their ability to scavenge and remove iron under in vivo conditions.

In contrast to **45** and **51**, the (hydroxyalkyl)pyridinone **50** is not converted to a carboxylate derivative nor rapidly glucuronidated.[35] These properties result in the molecule inducing a more prolonged period of iron excretion (Figure 6). Thus whereas iron excretion resulting from the oral administration of **27** is virtually complete 12 h after oral administration, with **50** excretion continues over the entire 24-h period. Indeed this compound was found to be the most efficient HPO tested (Table 5), being more effective than both Deferiprone (**27**) and desferrioxamine. However in the [^{59}Fe]ferritin model the activity of **50** was found not to be significantly different from that of Deferiprone (**27**) (Figure 7).

Thus, although the (hydroxyalkyl)pyridinone **50** may offer some advantages over the simple *N*-alkylhydroxy-pyridinones, the influence will probably be marginal. For treatment of thalassemia, delivery of such molecules to the liver is required, and ester prodrugs of (hydroxy-alkyl)pyridinones are currently under investigation.[39]

Experimental Section

General Procedure. Melting points are uncorrected. IR spectra were recorded on a Perkin-Elmer 298 IR spectrometer. Proton NMR spectra were determined with a Perkin-Elmer R32 (90 MHz) NMR spectrometer. Mass spectra (EI) or positive fast atom bombardment (FAB) were recorded on JEOL AX505W and KRATOS MS890 mass spectrometers. Elemental analyses were performed by Butterworth Laboratories Limited, Teddington, Middlesex, or Micro Analytical Laboratories, Department of Chemistry, The University of Manchester, Manchester. Full spectroscopic and analytical data are available as Supporting Information.

2-Methyl-3-(benzyloxy)-4-(1H)-pyranone, 3. To a stirred solution of maltol (**1**) (178.0 g, 1.41 mol) in methanol (1800 mL) was added sodium hydroxide (60 g, 1.5 mol) in water (200 mL) followed by benzyl chloride (209 g, 1.65 mol), and the mixture was heated to reflux for 12 h. After removal of solvent by rotary evaporation the resultant orange oil was taken up in dichloromethane (800 mL) and washed with 5% (w/v) aqueous sodium hydroxide (5 × 300 mL) and water (2 × 500 mL). The organic fraction was dried over anhydrous sodium sulfate and filtered. The solvent was removed by rotary evaporation to give a colorless oil which was triturated with diethyl ether and cooled at 0 °C for 1 h to give solid product. Recrystallization from diethyl ether afforded **3** as colorless needles (243 g, 83%): mp 56–57 °C (lit. value[17] 51–52 °C).

An analogous procedure using ethylmaltol (**2**) gave 2-ethyl-3-(benzyloxy)-4-(1H)-pyranone (**4**) (80%): mp 33–34 °C (lit. value[17] 33–34 °C).

1-Amino-2-methyl-2-propanol. Lithium aluminum hydride (12.5 g, 0.33 mol) was suspended in dry ether (200 mL) and cooled to 0 °C under a nitrogen atmosphere. Acetone cyanohydrin (13.35 g, 0.157 mol) in dry ether (50 mL) was added dropwise during 1 h, and the reaction mixture stirred overnight at room temperature. With continued cooling and vigorous stirring, water (12 mL), sodium hydroxide (20%, 9 mL), and water (40 mL) were added. The ether solution was decanted and the residue washed with ether (2 × 50 mL). The ether portions were all combined, dried over anhydrous sodium

sulfate, filtered, and concentrated in vacuo to yield a colorless oil[40] (7.24 g, 51.7%).

2-Amino-1,3-bis(benzyloxy)propane. 1,3-Bis(benzyloxy)-2-propanol (2.3 g, 8.4 mmol), triphenylphosphine (2.43 g, 9 mmol), and phthalimide (1.37 g, 9 mmol) were dissolved in dry tetrahydrofuran (40 mL) at room temperature under nitrogen atmosphere. Diethyl azodicarboxylate (1.62 g, 9 mmol) was then added. The resulting mixture was stirred at room temperature for 24 h. Solvent was removed at reduced pressure, and the product was purified by column chromatography (silica, eluant 20% EtOAc/petroleum ether, bp 40–60 °C) to give white crystals of 1,3-bis(benzyloxy)-2-phthalimidopropane (2.60 g, 70%): mp 82–83 °C. Anal. ($C_{25}H_{23}NO_4$) C, H, N.

To a solution of 1,3-bis(benzyloxy)-2-phthalimidopropane (4.60 g, 12 mmol) in absolute ethanol (60 mL) was added hydrazine hydrate (55%, 14.7 mL, 13 mmol), and the mixture refluxed for 3 h. The reaction mixture was cooled at 0 °C and acidified with concentrated hydrochloric acid (pH < 2). The resulting suspension was filtered and the collected phthalhydrazide washed with water (2 × 60 mL). The filtrate was evaporated to dryness under reduced pressure. The resulting residue was dissolved in water (100 mL), diethyl ether (100 mL) was added, and the aqueous layer was made alkaline (pH = 12) at 0 °C by addition of saturated potassium hydroxide. The resulting mixture was stirred at 0 °C for 30 min. The organic layer was separated, and the aqueous layer was extracted with diethyl ether (3 × 100 mL). The combined ether extracts were dried (Na$_2$SO$_4$), filtered, and concentrated in vacuo to dryness to yield 2-amino-1,3-bis(benzyloxy)propane as a yellow oil (2.80 g, 86%).

1-(2′-Methyl-2′-hydroxypropyl)-2-methyl-3-hydroxy-4(1H)-pyridinone, 47. Sodium hydroxide solution (10 M) was added to a mixture of benzylmaltol (**3**) (2.0 g, 9 mmol) in ethanol (25 mL), water (25 mL), and 1-amino-2-methyl-2-propanol (2.4 g, 27 mmol) until the mixture reached pH 13. The resulting suspension was heated under reflux for 12 h. After removal of the solvent by rotary evaporation, water (50 mL) was added, and the mixture was adjusted to pH 1 with concentrated hydrochloric acid and washed with diethyl ether (2 × 25 mL). The resultant aqueous solution was then adjusted to pH 7 with 10 M sodium hydroxide solution and extracted with dichloromethane (3 × 50 mL). The organic extracts were combined, dried over anhydrous sodium sulfate, and filtered. The solvent was removed by rotary evaporation to give a yellow solid. Recrystallization from ethanol/diethyl ether afforded 1-(2′-methyl-2′-hydroxypropyl)-2-methyl-3-(benzyloxy)-4(1H)-pyridinone (**8**) as a white powder (1.15 g, 45%): mp 153–154 °C. Anal. ($C_{17}H_{21}NO_3$) C, H, N.

To a solution of 1-(2′-methyl-2′-hydroxypropyl)-2-methyl-3-(benzyloxy)-4(1H)-pyridinone (**8**) (2.7 g, 10 mmol) in ethanol (90 mL) and water (10 mL) was added 5% palladium on charcoal catalyst (0.25 g). The mixture was stirred at room temperature under a constant stream of hydrogen for 24 h. After removal of used catalyst by filtration, the solution was boiled with activated charcoal and filtered. The solvent was removed by rotary evaporation to give a cream-colored solid. Recrystallization from ethanol/diethyl ether yielded 1-(2′-methyl-2′-hydroxypropyl)-2-methyl-3-hydroxy-4(1H)-pyridinone (**47**) as a white powder (1.50 g, 80%): mp 204–205 °C; ^{1}H NMR (DMSO-d_6) δ 1.1 (6H, s, 2 CH$_3$), 3.32 (3H, d, 2-CH$_3$), 3.86 (2H, s, NCH$_2$), 5.8–6.1 (2H, br, 2 OH), 6.14 (1H, d, 5-H), 7.55 (1H, d, 6-H). Anal. ($C_{10}H_{15}NO_3$) C, H, N.

Analogous syntheses reacting either **3** or **4** with 2-amino-1,3-bis(benzyloxy)propane, 3-aminopropan-1-ol, 4-aminobutan-1-ol, aminoacetaldehyde dimethyl acetal, and aminoacetaldehyde diethyl acetal gave 1-(1′-(benzyloxymethyl)-2-(benzyloxy)ethyl)-2-methyl-3-(benzyloxy)-4(1H)-pyridinone (**9**), 1-(3′-hydroxypropyl)-2-ethyl-3-(benzyloxy)-4(1H)-pyridinone (**10**), 1-(4′-hydroxybutyl)-2-ethyl-3-(benzyloxy)-4(1H)-pyridinone (**11**), 1-(2′,2′-dimethoxyethyl)-2-methyl-3-(benzyloxy)-4(1H)-pyridinone (**12**), and 1-(2′,2′-diethoxyethyl)-2-methyl-3-(benzyloxy)-4(1H)-pyridinone (**13**), respectively, as free base or hydrochloride salts on acidic workup.

Analogous hydrogenolysis procedure using **9**, **10**, and **11**–**13** varying the reaction period from 6 to 24 h afforded **49**, **51**–**52**, and **56**–**57**, respectively, as shown in Table 2.

1-(2′-Carboxyethyl)-2-ethyl-3-(benzyloxy)-4(1*H*)-pyridinone, 14. To a solution of **4** (23 g, 0.1 mol) in ethanol (300 mL) and water (300 mL) was added β-alanine (11.0 g, 0.12 mol) followed by 10 M sodium hydroxide solution until pH 13 was attained. After heating under reflux for 18 h, the resulting solution was reduced in volume (~100 mL) by rotary evaporation and water was added. The aqueous solution was adjusted to pH 9 by adding hydrochloric acid and washed with diethyl ether (2 × 100 mL) prior to adjustment to pH 4 (by adding hydrochloric acid) and extraction with dichloromethane (5 × 100 mL). The organic fractions were combined, dried over anhydrous sodium sulfate, and filtered. The solvent was removed by rotary evaporation to a yellow oil which was triturated with acetone and then solidified by cooling at −15 °C. Recrystallization from hot water/acetone yielded light-yellow crystals (21 g, 70%): mp 156–157 °C. Anal. ($C_{17}H_{19}$-NO_4) C, H, N.

Analogous procedure reacting **4** with 4-aminobutyric acid and **3** with β-alanine or 4-aminobutyric acid gave **15**, **16**, and **17**, respectively.

Analogous procedure using **3** and taurine at pH > 12 gave 1-(2′-sulfoxyethyl)-3-methyl-3-(benzyloxy)-4(1*H*)-pyridinone (**18**) in zwitterionic form (80%): mp > 300 °C. Anal. ($C_{15}H_{17}NO_5S$) C, H, N, S.

1-(2′-Carboxyethyl)-2-ethyl-3-hydroxy-4(1*H*)-pyridinone, 62. To a solution of **14** (1.5 g, 5 mmol) in tetrahydrofuran (30 mL) and water (20 mL) was added 2 drops of 1 M hydrochloric acid followed by 5% palladium on charcoal catalyst (0.2 g). The mixture was stirred at room temperature for 6 h under a constant stream of hydrogen. After removal of used catalyst by filtration, the solution was concentrated to dryness by rotary evaporation to give a cream-colored solid. Recrystallization from water yielded cream-colored crystals (0.91 g, 87%): mp 167–168 °C; ^{1}H NMR (DMSO-d_6) δ 1.12 (3H, t, CH$_2$**CH$_3$**), 2.68 (2H, t, CH$_2$CO$_2$-), 2.7 (2H, q, **CH$_2$**CH$_3$), 4.16 (2H, q, NCH$_2$), 6.15 (1H, d, 5-H), 6.8 (2H, br, s, 2OH), 7.6 (1H, d, 6-H). Anal. ($C_{10}H_{13}NO_4$) C, H, N.

Analogous procedure using **15** and **18** in aqueous ethanol gave **63** and **64**, respectively, as shown in Table 2.

1-[2′-(Methoxycarbonyl)ethyl]-2-methyl-3-hydroxy-4(1*H*)-pyridinone Hydrochloride, 65. A solution of methanol (0.5 g, 15 mmol) and triphenylphosphine (2.88 g, 11 mmol) in dry tetrahydrofuran (30 mL) was added to a solution of diethyl azodicarboxylate (1.92 g, 11 mmol) and **16** (2.88 g, 10 mmol) in dry tetrahydrofuran (100 mL) at room temperature. After the reaction mixture stirred for 16 h, the solvent was removed under reduced pressure. The residue was purified by column chromatography on silica gel (eluant 10% methanol in chloroform) to afford a light-yellow oil of 1-[2′-(methoxycarbonyl)ethyl]-2-methyl-3-(benzyloxy)-4(1*H*)-pyridinone (**19**) (2.65 g, 88%). The oily product was dissolved in dimethylformamide (50 mL) and subjected to hydrogenolysis reaction in the presence of 5% Pd/C (10% (w/w) of the compound) catalyst for 12 h. The mixture was warmed and filtered. The filtrate was acidified using hydrogen chloride gas followed by rotary evaporation to give a white solid. Recrystallization from methanol/diethyl ether gave a white powder (85%): mp 142–144 °C. Anal. ($C_{10}H_{14}NO_4Cl$) C, H, N, Cl.

Analogous synthesis using ethanol gave 1-[2′-(ethoxycarbonyl)ethyl]-2-methyl-3-(benzyloxy)-4(1*H*)-pyridinone (**20**) (92%). Hydrogenolysis procedure as above gave **66** (Table 2).

Route 1. Synthesis of Amides via Succinimide Active Ester. 1-[3′-((Succinimidyloxy)carbonyl)propyl]-2-methyl-3-(benzyloxy)-4(1*H*)-pyridinone, 7a. To a solution of 1-(3′-carboxypropyl)-2-methyl-3-(benzyloxy)-4(1*H*)-pyridinone (**17**) (5.7 g, 19 mmol) in dimethylformamide (100 mL) were added a solution of *N*-hydroxysuccinimide (2.3 g, 20 mmol) and dicyclohexylcarbodiimide (DCCI; 4.13 g, 20 mmol) each in dry dimethylformamide (25 mL). The resulting mixture was stirred in darkness at 0 °C for 1 h under an atmosphere of nitrogen and at room temperature for 16 h. After the dense

white precipitate was removed by filtration, dimethylformamide was removed by rotary evaporation under high vacuum to give an oil which was extracted into dichloromethane (200 mL) and washed with water (3 × 100 mL). The organic layer was dried over anhydrous sodium sulfate and filtered. The solvent was removed by rotary evaporation to give a light-yellow oil which was dissolved in ethyl acetate and cooled at 0 °C for 1 h to give a white solid. Recrystallization from ethyl acetate yielded white crystals (7.15 g, 95%): mp 99–101 °C; ^{1}H NMR (DMSO-d_6) δ 1.75–2.08 (2H, m, CH$_2$**CH$_2$**CH$_2$COO), 2.16 (3H, s, 2-CH$_3$), 2.73 (2H, t, CH$_2$CO), 2.83 (4H, s, succinimideCH$_2$), 3.95 (2H, t, NCH$_2$), 5.06 (2H, s, CH$_2$Ph), 6.23 (1H, d, 5-H), 7.2–7.5 (5H, m, ArH), 7.63 (1H, d, 6-H).

Analogous procedure using **14** gave 1-[2′-((succinimidyloxy)carbonyl)ethyl]-2-ethyl-3-(benzyloxy)-4(1*H*)-pyridinone (**7b**) as white crystals (66%): mp 165–166 °C.

1-[3′-(Methylcarbamoyl)propyl]-2-methyl-3-(benzyloxy)-4(1*H*)-pyridinone Hydrochloride, 21. Methylamine (2 g, 26 mmol, 40% in water) was added dropwise to a solution of **7a** (8.76 g, 22 mmol) in dichloromethane (200 mL). After the reaction mixture stirred overnight at room temperature, the solution was filtered, washed with water (3 × 100 mL), dried over anhydrous sodium sulfate, and filtered. The solvent was removed by rotary evaporation to give a colorless oil which was dissolved in ethanol, and hydrochloric acid was added. The product was reconcentrated to yield a white solid. Recrystallization from ethanol/diethyl ether yielded white crystals (7.2 g, 93%): mp 161–162 °C. Anal. ($C_{18}H_{23}N_2O_3Cl$) C, H, N, Cl.

Analogous procedure reacting 1-[2′-((succinimidyloxy)carbonyl)ethyl]-2-ethyl-3-(benzyloxy)-4(1*H*)-pyridinone (**7b**) with methylamine and propylamine gave **22** and **23** in yields of 40% and 55%, respectively.

Route 2. Synthesis of Amides via Benzotriazolyl Active Ester. 1-[2′-(Dimethylcarbamoyl)ethyl]-3-(benzyloxy)-2-ethyl-4(1*H*)-pyridinone Hydrochloride, 24. *N*-Methylmorpholine (2.80 g, 26 mmol) was added to a solution of 1-(2′-carboxyethyl)-2-ethyl-3-(benzyloxy)-4(1*H*)-pyridinone (**14**) (7.53 g, 25 mmol) in dimethylformamide (100 mL) followed by 2-(1*H*-benzotriazol-1-yl)-1,1,3,3-tetramethyluronium tetrafluoroborate (TBTU; 8 g, 25 mmol) under an atmosphere of nitrogen. After the reaction mixture stirred for 20 min at room temperature, dimethylamine (1.3 g, 25 mmol) was added dropwise and the mixture was stirred for 4 h. Dimethylformamide was removed, and the product was taken into dichloromethane (100 mL). The organic fraction was washed with 5% hydrochloric acid (2 × 50 mL), 5% aqueous sodium hydroxide (3 × 50 mL), and water (2 × 50 mL), dried over anhydrous sodium sulfate, filtered, and concentrated to give an oil which was dissolved in ethanol and hydrochloric acid. A white solid was obtained after removing the solvent by rotary evaporation. Recrystallization from ethanol/diethyl ether yielded a white powder (6.5 g, 72%): mp 147–148 °C. Anal. ($C_{19}H_{25}N_2O_3Cl$) C, H, N, Cl.

Analogous procedure using diethylamine, methylamine, and propylamine yielded **25**, **22**, and **23** in yields of 70%, 74%, and 73%, respectively.

1-[3′-(Methylcarbamoyl)propyl]-2-methyl-3-hydroxy-4(1*H*)-pyridinone Hydrochloride, 69. To a solution of 1-[3′-(methylcarbamoyl)propyl]-2-methyl-3-(benzyloxy)-4(1*H*)-pyridinone hydrochloride (**21**) (7 g, 20 mmol) in ethanol (100 mL) and water (25 mL) was added 5% Pd/C catalyst (0.8 g). The mixture was stirred at room temperature under a constant stream of hydrogen for 5 h. After used catalyst was removed by filtration, the solution was boiled with activated charcoal for 5 min and filtered. The solvent was removed by rotary evaporation to give a white solid. Recrystallization from ethanol/diethyl ether gave white crystals (4.9 g, 95%): mp 207–209 °C; ^{1}H NMR (D$_2$O, Ext TMS) δ 1.96–2.26 (2H, m, $^+$NCH$_2$**CH$_2$**CH$_2$CO), 2.36 (2H, t, CH$_2$CO), 2.59 (3H, s, 2-CH$_3$), 2.66 (3H, s, CONH**CH$_3$**), 4.38 (2H, t, $^+$NCH$_2$), 7.12 (1H, d, 5-H), 8.1 (1H, d, 6-H). Anal. ($C_{11}H_{17}O_3N_2Cl$) C, H, N, Cl.

Analogous hydrogenolysis procedure using **22**–**25** gave **76**–**79**, respectively, as shown in Table 2.

Determination of Distribution Coefficients Using the Filter Probe Method. 1. Free Ligands. Distribution coefficients were determined using an automated continuous flow technique similar to that described by Tomlinson.[26] The system was comprised of an IBM-compatible PC running the TOPCAT program,[41,42] which controlled both a Metrohm 665 Dosimat autoburet and a Pye-Unicam Lambda 5 UV/vis spectrophotometer, as well as performing all calculations of distribution coefficients. All distribution coefficient determinations were performed using AnalaR grade reagents under a nitrogen atmosphere using a flat-based glass vessel equipped with a sealable lid at 25 °C. The aqueous and octanol phases were presaturated with respect to each other before use. The filter probe consisted of a poly(tetrafluoroethylene) (PTFE) plunger associated with a gel-filtration column. The aqueous phase (50 mM MOPS buffer, pH 7.4, prepared using Milli-Q water) was separated from the two-phase system (1-octanol/ MOPS buffer, pH 7.4) by means of a hydrophilic cellulose filter (5-μm diameter, 589/3 Blauband filter paper, Schleicher and Schuell) mounted in the gel-filtration column adjuster (SR 25/ 50, Pharmacia). A known volume (normally 25−50 mL) of MOPS buffer (saturated with octanol) was taken in the flat base mixing chamber. After a baseline was obtained the solution was used for reference absorbance. A 1×10^{-4} M solution of the ligand was prepared in the aqueous phase (typically 50 mL) to give an absorbance of between 0.5 and 1.5 absorbance units at the preselected wavelength ($\sim$280 nm). The flow rate of the aqueous circuit was limited to 1 mL m^{-1}. The computer program was initiated. When a constant absorbance was obtained (defined as an absorbance change of less than 0.002 absorbance unit over a minimum of 100 individual readings) a suitable aliquot of 1-octanol was added to the aqueous phase from the automatic dispenser. The two immiscible phases were continuously stirred to ensure effective partitioning of the sample compound. Subsequent absorbance readings were recorded until the system reached equilibrium when a further aliquot of 1-octanol was added. The cycle was repeated for at least five additions of 1-octanol. An estimate of the distribution coefficient was obtained from each 1-octanol addition, which enabled calculation of a mean distribution coefficient value and standard deviation.

2. Iron(III) Complexes. Distribution coefficients were measured using a 10:1 molar ratio of ligand to iron to ensure that the 3:1 neutral complexes formed. The ligand was dissolved in 10 mL of MOPS buffer (pH 7.4) to give a stock solution with a concentration of 0.1 M. Iron(III) nitrate nonahydrate was dissolved in 10 mL of HCl (0.1 M) at a concentration of 0.1 M. The iron(III) complexes were prepared in the glass vessel by the addition of 400 μL of ligand solution to 39.56 mL of MOPS buffer, and then the iron solution (40 μL) was added to give a total volume of 40 mL resulting in concentrations of ligand and iron of 10^{-3} and 10^{-4} M, respectively. Absorbance of the iron(III) complexes was monitored at 460 nm (λ_{max}). The partitioning was carried out as described above.

Molecular Modeling. The structure of the iron(III)−**50** complex was obtained by energy minimization procedures using the Polak-Ribiere algorithm of Hyper Chem program; Hyper Chem (Release 2) for Silicon Graphics (Hypercube), 1992.

Determination of Distribution Coefficient Values Using the Shake-Flask Method. The distribution coefficients of the iron(III) complexes with values greater than 100 were monitored using MOPS buffer/1-octanol volume ratio of 100:1 at 25 °C. In contrast, for both ligands and iron(III) complexes which possess distribution coefficient values less than 0.01, MOPS buffer/1-octanol volume ratio of 1:100 was used.[27] A solution of ligands with concentration of 10^{-4} M was prepared in MOPS buffer (pH 7.4), and the absorbance of the solution was measured in the ultraviolet region at a wavelength of approximately 289 nm using the buffer as a blank. A 10-mL sample of the solution was stirred vigorously with 1000 mL of 1-octanol in a glass vessel for 1 h. The two layers were separated by centrifugation at 3000 rpm for 5 min. An aliquot

of the aqueous layer was then carefully removed using a glass Pasteur pipet ensuring that the sample was not contaminated with 1-octanol. The distribution coefficient was calculated from the ratio of the equilibrium absorbance to the decrease in absorbance of the aqueous phase. For each sample, the experiment was repeated at least four times which led to calculation of a mean distribution coefficient value and standard deviation.

Determination of Physical Constants of Ligands. 1. pK_a Determination. Equilibrium constants of protonated ligands were determined using an automated computerized system, consisting of a Metrohm 665 dosimat, a Perkin-Elmer λ5 UV/vis spectrophotometer, a Corning ion analyzer 225, and a 286 Opus PC which controlled the integrated system.[25] A combined Sirius electrode was used to calibrate the electrode zero and to measure pH values. This system is capable of undertaking simultaneous spectrophotometric and potentiometric measurements. A blank titration of 0.1 M KCl (25 mL) was carried out to determine the electrode zero using Gran's plot method.[43] The solution (0.1 M KCl, 25 mL), contained in a jacketed titration cell, was acidified by 0.15 mL of 0.2 M HCl. Titrations were carried out against 0.3 mL of 0.2 M KOH using 0.01-mL increments dispensed from a Metrohm 665 dosimat. Solutions were maintained at 25 $\pm$ 0.5 °C under an argon atmosphere. The above titration was repeated in the presence of ligand. The data obtained from titrations were analyzed by the TITRFIT program, a modified version of NONLIN15.[25] The pK_a values were obtained to an accuracy of $\pm$0.02 pH unit.

2. Iron(III) Affinity Constant Determination. The K_i value for the iron(III)−ligand interaction was determined by a spectrophotometric competition study of ligand−Fe(III)− EDTA using the automated system.[42] The iron(III) complexes of the ligand were prepared in 5:1 molar ratio in 0.1 M 3-(*N*-morpholino)propanesulfonic acid (MOPS) buffer, pH 7.4. This solution was then titrated against EDTA. The resulting spectrophotometric data were inserted into the COMPT1 program to evaluate the affinity constants of the complex. Affinity constants were obtained to an accuracy of $\pm$0.02 log unit. Speciation plots were obtained by running the program MLCOM50.[25] These programs require concentrations of metal and ligand, K_i(Fe^{III}) values of complexes, K_i values for the Fe^{III}−OH interaction, and pK_a value of ligand.

Biological Methods. The guidelines provided by the Home Office (Animals (Scientific Procedures) Act 1986) were adopted throughout this study.

1. Excretion of Iron in Bile. In vivo testing of HPOs was carried out in non-iron-overloaded, bile duct-cannulated rats.[28] Male rats (Fischer) weighing 200−240 g were switched from standard rodent food (Nafag 890 rat maintenance diet; Gossau, Switzerland) to an iron-poor diet (Nafag 9046) 5 days prior to the start of the test. One day before surgery, the animals were fasted and adapted to metabolic cages where drinking water was freely accessible.

Rats were anesthetized by inhalation of 4% isofluane (Forene, Abbott) mixed with oxygen. After complete anesthetization, the animal body was transferred to an operation table and the concentration of isofluane reduced to about 2%. The abdomen and shoulder areas were shaved and sterilized with 70% ethanol. The abdominal cavity was opened by an incision of 2 cm allowing the stomach and duodenum to be visualized, after retraction of the abdominal wall. After locating the bile duct leading from the liver to the duodenum, forceps were used to free the duct from surrounding connective tissue. A small opening was made in the duct about 1 cm from the duodenum using iris scissors. A cannula was prepared by cutting polyethylene tubing (Portex, U.K.; i.d. 0.58 mm, o.d. 0.96 mm) at an angle to leave a bevel point. The cannula was carefully inserted 1.5 cm into the bile duct. After bile flow was established the cannula was tied snugly in place with surgical thread. The cannula was further secured by placing a second suture below the insertion. The abdominal layer was then closed with thread, allowing the collection tubing to emerge from the lower end of the incision. A skin tunneling needle was inserted at the shaved shoulder area and fed around to

the abdominal incision. The collection tubing was threaded through the needle until it emerged from the shoulder opening. The needle was then removed and the abdominal dermal flaps closed with surgical thread. The collection tubing was passed through a rodent jacket (Harvard Instruments) worn around the chest to a miniature single channel fluid swivel inside a metal torque-transmitting tether. The animal was observed at 30 °C constant temperature under an infrared lamp for 30 min and its bile collected in a 10-mL plastic tube.

Rats were transferred back to their individual metabolic cages. The collection tubing was directed from the animal to a fraction collector by a fluid swivel mounted above the metabolic cage. This system allowed the animal to move freely in the cages while continuous bile samples were collected. Control samples of bile and urine were collected for 3 h. After administration of the test compound (subcutaneously or by gavage), bile samples were collected in plastic disposable tubes for 24 h at 3-h intervals and urine was collected for 24 h. To reduce postoperative pain, the rats received three subcutaneous doses of Temgesic (Reckitt & Colman, Hull, England) (the first immediately after operation, the second 5 h after operation, and the third 16 h later, each 0.6 mL/kg of body weight). Temgesic contains the long-acting and potent analgesic buprenorphine. Food was given ad libitum 2 h after the drug application.

At the end of the experiment, animals were sacrificed with CO_2. The volume of each bile and urine fraction was measured, and the samples were stored at -20 °C until determination of their iron concentration.

2. Bile and Urine Iron Assay. Iron concentration in bile and urine was determined colorimetrically using the Bathophenanthrolin method.[44] Experimental operations were performed with the aid of a Biomek 2000 pipet robot (Beckman).

Bile and urine were briefly vortexed, and 0.1 mL of each sample was pipetted twice into two wells of a conical-bottom microplate (96 wells; Nunc, Denmark). Water and standard iron solution (10 μg/mL and 20 μg/mL; Janssen Chimica, Belgium) were included on each plate. To each well, 0.1 mL of acid solution (10% TCA, 3 M HCl) was added with an Eppendorf multipipet. After incubation in a 65 °C bath for 4 h, the 96-well plates were centrifuged for 10 min at 2000g (2500 rpm, Omnifuge 2.ORS; Heraeus). A portion of each supernatant (0.1 mL) was automatically transferred (Biomek 2000, Beckman) to the corresponding well of the flat-bottom microplate (Dynatech). Then 0.1 mL of iron indicator solution (9.48 mL of H_2O, 120 μL of mercaptoacetic acid, 18.6 mg of bathophenanthrolin sulfonate, 4.74 mL of saturated sodium acetate, and 6.33 mL of NaOH, 5.9 M) was added. Blank solution (no color reagent bathophenanthrolin) was also pipetted to another well. The plates were agitated for 30 min, and the absorbance was measured at 535 nm with a Biomek plate reader. The iron concentration of each sample was estimated by comparison with the standard solutions after subtraction of individual blank absorbance. Calculation was performed on a Macintosh computer using the Excel software.

3. Method of Iron Mobilization Efficacy Study in Rats. Hepatocytes of normal fasted rats (190–230 g) were labeled with ^{59}Fe by administration of [^{59}Fe]ferritin via the tail vein. One hour later, each rat was administered orally with chelator (450 μmol/kg). Control rats were administered with an equivalent volume of water. The rats were placed in individual metabolic cages and urine and feces collected. Rats were allowed access to food 1 h after oral administration of chelator. There was no restriction of water throughout the study period. The investigation was terminated 24 h after the [^{59}Fe]ferritin administration, rats were sacrificed and the liver and gastrointestinal tract (including its content and feces) were removed for gamma counting.

Supporting Information Available: Full elemental and spectral analyses of compounds **8**–**25** and **47**, **49**, **51**, **52**, **56**, **57**, **62**–**66**, **69**, and **76**–**79** (14 pages). Ordering information is given on any current masthead page.

References

(1) Halliwell, B.; Gutteridge, J. M. C. *Free Radicals in Biology and Medicine*, 2nd ed.; Clarendon Press: Oxford, 1998; pp 22–85.

(2) Barton, J. C.; Bertoli, L. F. Hemochromatosis: The genetic disorder of the twenty-first century. *Nature Med.* **1996**, *2*, 394–395.

(3) Pippard, M. J. Secondary Iron Overload. In *Iron Metabolism in Health and Disease*; Brock, J. H., Halliday, J. W., Pippard, M. J., Powell, L. W., Eds.; W. B. Saunders Co. Ltd.: London, 1994; pp 271–309.

(4) Hider, R. C.; Choudhury, R.; Rai, B. L.; Dekhordi, L. S.; Singh, S. Design of Orally active iron chelators. *Acta Haematol.* **1996**, *95*, 6–12.

(5) Hershko, C. Iron Chelators in Medicine. *Mol. Aspects Med.* **1992**, *13*, 114–165.

(6) Raymond, K. N.; Müller, G.; Maczanke, B. Complexation of iron by siderophores: A review of their solution and structural chemistry and biological function. *Top. Curr. Chem.* **1984**, *123*, 49–102.

(7) Martell, A. E.; Motekaitis, R. J.; Murase, I.; Sala, L. F.; Stoldt, R.; Ng, C. Y. Development of iron chelators for Cooley's Anaemia. *Inorg. Chim. Acta* **1987**, *138*, 215–230.

(8) Porter, J. Oral iron chelators: Prospects for future development. *Eur. J. Haematol.* **1989**, *43*, 271–285.

(9) Hider, R. C.; Porter, J. B.; Singh, S. The design of therapeutically useful iron chelators. In *The Development of Iron Chelators for Clinical Use*; Bergeron, R. J., Brittenham, G. M., Eds.; CRC Press: Ann Arbor, 1994; pp 353–371.

(10) (a) Martell, A. E.; Motekaitis, R. J.; Clarke, E. T. Synthesis of *N*,*N*′-di(2-hydroxybenzyl)ethylenediamine-*N*,*N*′-diacetic acid (HBED) derivatives. *Can. J. Chem.* **1986**, *64*, 449–456. (b) Hershko, C.; Grady, R. W.; Link, G. Phenolic ethylenediamine derivatives: A study of orally effective iron chelators. *J. Lab. Clin. Med.* **1984**, *103*, 337–346.

(11) Hider, R. C.; Hall, A. D. Clinically useful chelators of tripositive elements. *Prog. Med. Chem.* **1991**, *28*, 31–173.

(12) Anderegg, G.; Raber, M. Metal complex formation of a new siderophore desferrithiocin and of three related ligands. *J. Chem. Soc., Commun.* **1990**, 1194–1196.

(13) Garrett, T. M.; Miller, P. W.; Raymond, K. N. 2,3-Dihydroxyterephthalamides: Highly efficient iron(III)-chelating agents. *Inorg. Chem.* **1989**, *28*, 128–133.

(14) Orama, M.; Tilus, O.; Taskinen, J.; Lotta, T. Iron(III)-chelating properties of the novel catechol O-methyl inhibitor entacapone in aqueous solution. *J. Pharm. Sci.* **1997**, *86*, 827–831.

(15) Brittenham, G. M. Development of iron-chelating agents for clinical use. *Blood* **1992**, *80*, 569–575.

(16) Singh, S.; Epemolu, R. O.; Dobbin, P. S.; Tilbrook, G. S.; Ellis, B. L.; Damani, L. A.; Hider, R. C. Urinary metabolic profiles in human and rat of 1,2-dimethyl and 1,2-diethyl-substituted-3-hydroxypyridin-4-ones. *Drug Met. Disp.* **1992**, *20*, 256–261.

(17) Dobbin, P. S.; Hider, R. C.; Hall, A. D.; Taylor, P. D.; Sarpong, P.; Porter, J. B.; Xiao, G.; van der Helm, D. Synthesis, physicochemical properties, and biological evaluation of *N*-substituted-2-alkyl-3-hydroxy-4(1*H*)-pyridinones: Orally active iron chelators with clinical potential. *J. Med. Chem.* **1993**, *36*, 2448–2458.

(18) Le Blanc, D. T.; Akers, H. A. Maltol and ethyl maltol. *Food Technol. (Chicago)* **1989**, *43*, 78–84.

(19) Amundsen, L. H.; Nelson, L. S. Reduction of nitriles to primary amines with lithium aluminium hydride. *J. Am. Chem. Soc.* **1951**, *73*, 242–244.

(20) Mitsunobu, O.; Wada, M.; Sano, T. Stereospecific and stereoselective reactions 1. Preparation of amines and alcohols. *J. Am. Chem. Soc.* **1972**, *94*, 679–680.

(21) Mitsunobu, O. The use of diethyl azodicarboxylate and triphenylphosphine in synthesis and transformation of natural products. *Synthesis* **1981**, *1*, 1–28.

(22) Mitsunobu, O.; Yamada, Y. Preparation of esters of carboxylic acid phosphoric acid via phosphonium salts. *Bull. Chem. Soc. Jpn.* **1967**, *40*, 2380–2382.

(23) Dourtoglou, V.; Ziegler, J. C.; Gross, B. L1 Hexafluorophosphate De *O*-benzo-triazolyl-*N*,*N*-tetramethyl uronium. *Tetrahedron Lett.* **1978**, *15*, 1269–1272.

(24) Dourtoglou, V.; Gross, B. *O*-Benzo-triazolyl-*N*,*N*,*N*-tetramethyl uronium hexafluorophosphate as coupling reagent for the synthesis of peptides of biological interest. *Synthesis* **1984**, *7*, 572–574.

(25) Taylor, P. D.; Morrison, I. E. G.; Hider, R. C. Microcomputer application of nonlinear regression analysis to metal−ligand equilibria. *Talanta* **1988**, *35*, 507−512.

(26) Tomlinson, E. Filter-probe extractor. A tool for the rapid determination of oil−water partition coefficients. *J. Pharm. Sci.* **1982**, *71*, 602−604.

(27) Ellis, B. L.; Duhme, A. K.; Hider, R. C.; Hossain, M. B.; Rizvi, S.; van der Helm, D. Synthesis, physicochemical properties, and biological evaluation of hydroxypyranones and hydroxypyridinones: Novel bidentate ligands for cell-labeling. *J. Med. Chem.* **1996**, *39*, 3659−3670.

(28) Bergeron, R. J.; Wiegand, J. B.; Dionis, J. B.; Egli-Karmakka, M.; Frei, J.; Huxley-Tencer, A.; Peter, H. H. Evaluation of desferrithiocin and its synthetic analogues as orally effective iron chelators. *J. Med. Chem.* **1991**, *34*, 2072−2078.

(29) Pippard, M. J.; Johnson, D. K.; Finch, C. A. A rapid assay for evaluation of iron-chelating agents in rats. *Blood* **1981**, *58*, 685−692.

(30) Hershko, C.; Cook, J. D.; Finch, C. A. Storage iron kinetics III. Study of desferrioxamine action by selective radioiron labels of RE and parenchymal cell. *J. Lab. Clin. Med.* **1973**, *81*, 876−886.

(31) Ma, R.; Reibenspies, J. J.; Martell, A. E. Stabilities of 1,2-diethyl-3-hydroxy-4-pyridinone chelates of divalent and trivalent metal ions. *Inorg. Chim. Acta* **1994**, *223*, 21−29.

(32) Hider, R. C.; Taylor, P. D.; Walkinshaw, M.; Wang, J. L.; van der Helm, D. Crystal structure of 3-hydroxy-1,2-dimethylpyridin-4(1*H*)-one. An iron(III) chelation study. *J. Chem. Res.* **1990**, 316−317.

(33) Edward, J. T. Iron transport across biological membranes; Some fundamental considerations. In *Intestinal absorption of metal ions, trace metals and radionucleotides*; Skoryna, S. C., Edward, D. M., Eds.; Pergamon Press: Oxford, 1970; pp 8−26.

(34) Edward, J. T.; Ponka, P.; Richardson, D. R. Partition coefficients of the iron(III) complexes of pyridoxal isonicotinoyl hydrazone and its analogues and the correlation to iron chelation efficacy. *Biometals* **1995**, *8*, 209−217.

(35) Singh, S.; Choudhury, R.; Epemolu, R. O.; Hider, R. C. Metabolism and pharmacokinetics of 1-(2′-hydroxyethyl)- and 1-(3′-hydroxyethyl)-2-ethyl-3-hydroxypyridin-4-ones in the rat. *Eur. J. Drug Metab. Pharmacokinet.* **1996**, *21*, 33−41.

(36) Hider, R. C. Potential protection from toxicity by oral iron chelators. *Toxicol. Lett.* **1995**, *82/83*, 961−967.

(37) Molenda, J. J.; Jones, M. M.; Basinger, M. A. Enhancement of iron excretion via monoanionic 3-hydroxypyridin-4-ones. *J. Med. Chem.* **1994**, *37*, 93−98.

(38) Hider, R. C.; Lerch, K. The inhibition of tyrosine by pyridinones. *Biochem. J.* **1989**, *257*, 289−290.

(39) Choudhury, R.; Epemolu, R. O.; Rai, B. L.; Hider, R. C.; Singh, S. Metabolism and pharmacokinetics of 1-(2′-trimethylacetoxy-ethyl)-2-ethyl-3-hydroxypyridin-4-one (CP117) in the rat. *Drug Metab. Dispos.* **1997**, *25*, 332−339.

(40) Pollock, J. R. A.; Stevens, R. *Dictionary of organic compounds*, 4th ed.; Eyre and Spottiswoode Ltd.: London, 1965; Vol. 1, p 162.

(41) Hall, A. TOPCAT program for Determination of distribution coefficients. Department of Pharmacy, King's College London, U.K., 1990.

(42) Khodr, H. KDHK94 Program (a modified version of TOPCAT Program) for determination of distribution coefficients. Department of Pharmacy, King's College London, U.K., 1994.

(43) Gran, G. Determination of the equivalence point in potentiometric titrations. *Analyst* **1952**, *77*, 661−671.

(44) Smith, G. F.; McCurdy, W. H.; Diehl, H. The colorimetric determination of iron in raw and treated municipal water supplies by use of 4:7-diphenyl-1:10-phenanthroline. *Analyst* **1952**, *77*, 418−422.

(45) Kontoghiorghes. G. J.; Barr, J.; Nortey, P.; Sheppard, L. Selection of a new generation of orally active α-ketohydroxypyridine iron chelators intended for use in the treatment of iron overload. *Am. J. Haematol.* **1993**, *42*, 340−349.

(46) Nelson, W. O.; Karpishin, T. B.; Rettig, S. J.; Orvig, C. Physical and structural studies of *N*-substituted-3-hydroxy-2-methyl-4(1*H*)-pyridinones. *Can. J. Chem.* **1988**, *66*, 123−131.

(47) Zhang, Z.; Rettig, S. J.; Orvig, C. Lipophilic coordination compounds: aluminium, gallium, indium complexes of 1-aryl-3-hydroxy-2-methyl-4-pyridinones. *Inorg. Chem.* **1991**, *30*, 509−515.